355.
3. Voge, H. H.; Wagner, C. D.; Stevenson, D. P. *J. Catal.* **1963**, *2*, 58.
4. Adams, C. R.; Jennings, T. J. *J. Catal.* **1963**, *2*, 63.
5. Davydov, A. A.; Mikhaltchenko, V. G.; Sokolovskii, V. D.; Boreskov, G. K. *J. Catal.* **1978**, *55*, 299.
6. Shultz, K. H.; Cox, D. F. *J. Catal.* **1993**, *143*, 464.
7. (a) Lunsford, J. H. *Catal. Rev.* **1973**, *8*, 135. (b) Che, M.; Tench, A. *J. Adv. Catal.* **1983**, *32*, 1.
8. Losee, D. B. *J. Catal.* **1977**, *50*, 545.
9. Berger, P. A.; Roth, J. F. *J. Phys. Chem.* **1967**, *71*, 4307.
10. The hyperfine splittings for ^{17}O atoms can be resolved into isotropic parts and anisotropic parts as

$$\begin{bmatrix} 0 & & \\ & 0 & \\ & & -28 \end{bmatrix} = -28/3 + \begin{bmatrix} 28/3 & & \\ & 28/3 & \\ & & -56/3 \end{bmatrix} \text{ and}$$

$$\begin{bmatrix} 0 & & \\ & 0 & \\ & & -117 \end{bmatrix} = -117/3 + \begin{bmatrix} 117/3 & & \\ & 117/3 & \\ & & -234/3 \end{bmatrix}, \text{ respectively.}$$

The total spin density in O_2^- is $(-28/3)/(-1651)+(-28/3)/(-51.38)+(-117/3)/(-1651)+(-117/3)/(-51.38)=0.97$.[7b]
11. Miller, D. J.; Haneman, D. *Phys. Rev. B.* **1971**, *3*, 2918.
12. Eley, D. D.; Zammitt, M. A. *J. Catal.* **1971**, *21*, 366.
13. Wang, K. M.; Lunsford, J. H. *J. Phys. Chem.* **1969**, *73*, 2069.
14. Che, M.; McAteer, J. C.; Tench, A. J. *Chem. Phys. Lett.* **1975**, *31*, 145.
15. Ben Taarit, Y.; Lunsford, J. H. *J. Phys. Chem.* **1973**, *77*, 780.
16. Sabbadini, M. G. B.; Gervasini, A.; Morazzoni, F.; Strumulo, D. *J. Chem. Soc., Faraday Trans. 1*, **1987**, *83*, 2271.
17. Lumpov, A. I.; Mikheikin, I. D.; Zhidomirov, G. M.; Kazanskii, V. B. *Kinet. Katal. (Eng. transl.)*, **1978**, *19*, 1265.

Nonnegligible Dynamical Consequences of Vibration-Pseudorotation Coupling in a Symmetric Triatomic Molecule

Jae Shin Lee

Department of Chemistry, College of Natural Sciences, Ajou University, Suwon 441-749, Korea

Received May 3, 1995

It is well known that vibration-rotation interaction becomes an important factor for understanding the spectra and dynamical behavior in polyatomic molecules as the total angular momentum of the system increases.[1-4] For the states with zero total angular momentum, it is generally assumed that vibration-rotation coupling is very negligible and most treatments on vibration-rotation interaction usually ignore the effect of coupling terms in the kinetic energy operator.[5,6] However, there has been no systematic investigation on the effects of these coupling terms on the dynamics of polyatomic molecules as the molecular vibrational energy goes into higher regime. Since the angular momentum of the system can also be induced by the simultaneous vibrations, there could exist a coupling between vibration and rotation even for so called "rotationless" states ($J=0$) and the coupling effect may not be negligible in some highly excited levels. In this report, we present the case for which vibration-rotation coupling for $J=0$ (which will be called vibration-pseudorotation coupling) plays a nonnegligible role in destroying regular mode structure of the vibrational wavefunction in triatomic molecules.

The theoretical method and technique employed in this study were presented in detail in previous paper.[7] In short, the vibration-rotation Hamiltonian for a symmetric triatomic molecule derived in arbitrary mode coordinate[8] was used with the model potential function which can represent the real molecular potential surfaces reasonably. The Hamiltonian then was divided by pure vibrational (unperturbed) part and vibration-rotation coupling (perturbation) part. Therefore, the Hamiltonian operator was written as

$$H=H_0+T_{V\text{-}R}$$

where H_0 is pure vibrational Hamiltonian including potential and $T_{V\text{-}R}$ represents the coupling between vibration and rotation in the kinetic energy operator. The model potential function for a symmetric triatomic molecule with slight barrier to linearity was devised in Ref. 9 and developed further to include important coupling terms between vibrational modes in the expansion. In our case, the model potential function was expanded as

$$V(\eta_s, \eta_a, \eta_b)=c_s f_s^2+c_a f_a^2+x_1 f_b^2+x_2 f_b^4+x_3 f_s f_b^2+\varepsilon f_s f_a^2$$

The stretching coefficients, c_s and c_a, are given initially with

Table 1. Expansion coefficients for the model potential function of an ABA triatomic molecule

$V(\eta_s, \eta_a, \eta_b)=c_s f_s^2+c_a f_a^2+x_1 f_b^2+x_2 f_b^4+x_3 f_s f_b^2+\varepsilon f_s f_a^2$

$f_i=\dfrac{\tanh(a_i\eta_i)}{a_i}$; $i=a, b$ $\quad f_i=\dfrac{1-\exp(-a_i\eta_s)}{a_i}$; $i=s$

atomic mass	m_A=mass of ^1H, m_B=mass of ^{12}C
potential parameter	$a_s=0.8$ $a_b=6.0$ $a_a=1.4$
reference configuration[a]	$r^0=1.065$ A^0 $\theta_0=180°$
equilibrium configuration[b]	$r_e=1.070$ A^0 $\theta_e=136°$
barrier height to linearity	1000 cm^{-1}
expansion coefficients[c]	
c_s	0.3484798
c_a	65.17453
x_1	−2.965045
x_2	1364.669
x_3	35.06913
ε	−52.19362

[a] r^0 is the bond length between atom B and atom A in the linear saddle point geometry defined in Ref. 5. [b] r_e is the equilibrium bond length between atom B and atom A. [c] In units of hartree/(A^0)^n, where $n=2$ for c_s, c_a, x_1; $n=4$ for x_2; and $n=3$ for x_3, ε.

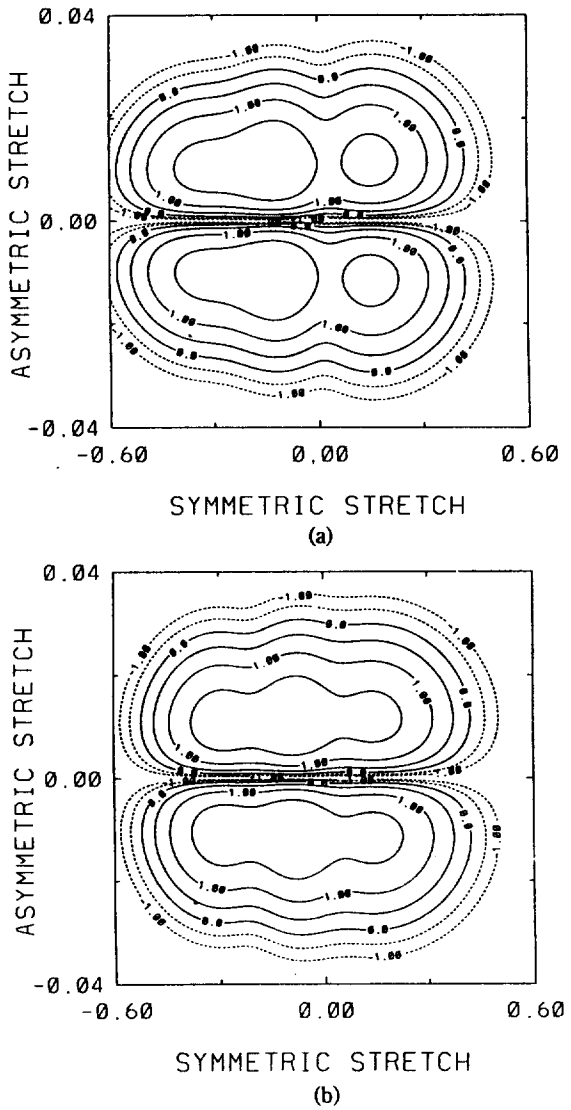

Figure 1. Contour plots of the square of the wavefunctions of (1 2 1) state for model potential in the symmetric and asymmetric stretch coordinate. (a) without and (b) with vibration-rotation coupling terms in the Hamiltonian. Values of common logarithm are plotted with contour interval of 0.5 in these figures. Dotted lines represent the negative values. The vibrational assignment is (symmetric stretch, bend, asymmetric stretch).

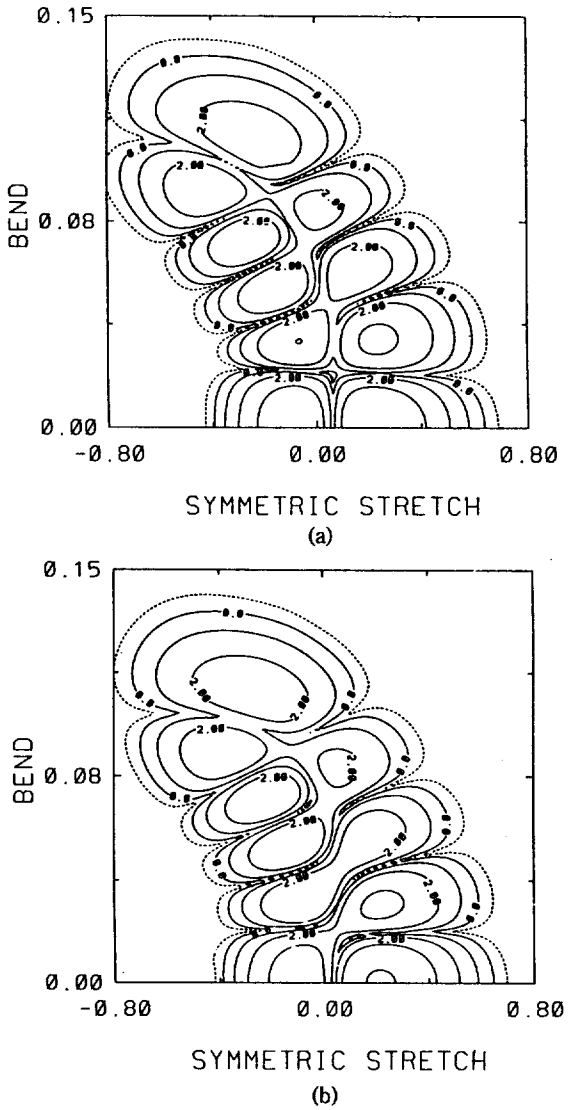

Figure 2. Contour plots of the square of the wavefunctions of the (1 4 1) state for real potential function of CH_2^+ in the symmetric stretch and bend coordinate. (a) without and (b) with vibration-rotation coupling terms in the Hamiltonian. Values of common logarithm are plotted with contour interval of 1.0 in these figures.

atomic masses, equilibrium geometry and barrier height to linearity. The bending coefficients (x_1, x_2, x_3) are automatically determined from the conditions that model potential function should satisfy. The stretching coupling coefficient ε was chosen for the potential function to give reasonable (positive) asymptotic behavior. f_i ($i=s$, a, b) is an appropriate function of vibrational coordinate which can represent the triatomic molecular potential surface more realistically. In our choice hyperbolic tangent function was employed for bend and asymmetric stretch mode, while Morse oscillator-type function was used for symmetric stretch mode with appropriate parameters. In Table 1 we give the data for the model potential function. Although this type of model potential function does not show the correct dissociation channel, it was shown that it can simulate the potential surfaces of real triatomic molecules very well in the bound state region by optimizing the parameters.[7,9,10] Using this model potential function, fully converged quantum variational calculations werecarried out both with H and H_0 which yielded in accurate energies and wavefunctions for unperturbed (pure vibrational) and perturbed (vibration-rotation interaction included) model CH_2 system, respectively. All states were converged to the point that adding further basis functions changed the energy by less than 0.5 cm^{-1}. Obtained wavefunctions were then used to investigate the changes in the vibrational structure induced by vibration-pseudorotation coupling. This was done by plotting contours of squares of wavefunctions in the vibrational coordinates integrated over remaining vibrational mode and rotational angles. For example, in symmetric stretch-bend

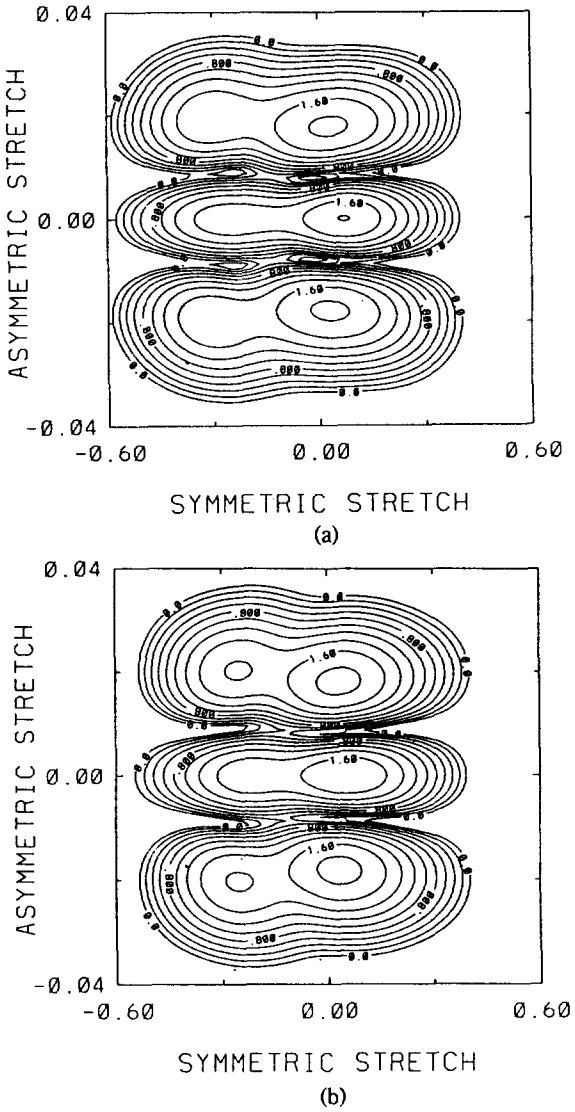

Figure 3. Contour plots of the square of the wavefunctions of the (0 3 2) state for real potential function of CH_2^+ in the symmetric and asymmetric stretch coordinate. (a) without and (b) with vibration-rotation coupling terms in the Hamiltonian. Values of common logarithm are plotted with contour interval of 0.2 in these figures.

coordinate plotting, square of wavefunction was integrated over asymmetric stretch coordinate as well as rotational angles.

For most levels with $J=0$ it was shown that inclusion or omission of the vibration-rotation coupling terms in the Hamiltonian did not affect the vibrational structure appreciably as expected. However, it also was found that the vibration-rotation coupling terms could noticeably affect the mode structure in some high energy states even with $J=0$ in certain cases. For example, for (1 2 1) level, which lies at 13163 cm^{-1} above the bottom of the potential well, the contour plot of the wavefunction without vibration-rotation coupling terms shows a more distinguishable mode structure in the symmetric-asymmetric stretch coordinate in Figure 1(a), while it is shown in Figure 1(b) that the breakdown of the symmetric stretch mode structure is more obvious as the coupling is switched on to the Hamiltonian. This could be a good example of demonstrating the importance of vibration-rotation coupling in highly excited states with $J=0$. The effects of coupling terms appeared to be more significant for the combination states than states of singly excited mode. At further higher vibrational energies, however, the mode structure of wavefunction would be eventually broken by mode coupling terms in the potential function (anharmonicity).

The nonnegligible role of vibration-pseudorotation coupling in destroying the mode structure of vibrational wavefunctions was also examined in realistic molecular potential of CH_2^+ which has a similar equilibrium geometry and barrier height to linearity as the model potential function. The potential function was obtained by fitting ab initio potential surface by Bartholomae *et al.*[11] to SPF (Simons-Parr-Finlan) type functions.[12,13] Same variational calculations were performed for the realistic potential of CH_2^+ molecule. As in case of the model potential, for most levels with $J=0$, no significant change in vibrational structure was noticed by the inclusion of vibration-pseudorotation coupling. However, in some combination levels, such as (1 4 1) and (0 3 2) which lie at 13713 cm^{-1} and 12933 cm^{-1} above the bottom of the well, the effect of vibration-pseudorotation coupling on wavefunction made a clear difference in vibrational structure, which is shown in Figure 2 and Figure 3. It is clear that mode mixing is developed between the symmetric stretch and bend mode as the coupling is switched on in Figure 2(b). Meanwhile, in Figure 3(b), the vibration-pseudorotation coupling further distorts already loosened mode structure by providing another maximum of probability density along the symmetric stretch coordinate. It should be noted, however, that the vibrational spectra and dynamical behavior of real CH_2^+ molecule in the ground electronic state would be significantly affected by the vibronic interaction (Renner-Teller effect).[14] The detailed analysis of the effects of vibration-pseudorotation coupling on vibrational spectra and structure in various type of triatomic molecules will be presented elsewhere.[10]

Acknowledgment. The author acknowledges the System Engineering Research Institute in Daeduk, Korea for an allocation of computer time on Cray C90, where most of calculations were performed. This work was supported by the grant from the Korea Science and Engineering Foundation.

References

1. Dai, H. L.; Korpa, C. L.; Kinsey, J. L.; Field. R. W. *J. Chem. Phys.* **1990**, *82*, 1688.
2. Silbert, E. L. *J. Chem. Phys.* **1989**, *90*, 2672.
3. Aoyagi, M.; Gray, S. K. *J. Chem. Phys.* **1991**, *94*, 195.
4. Sumpter, B. G.; Martens, C. C.; Ezra, G. S. *J. Phys. Chem.* **1988**, *92*, 7193.
5. Carney, G. D.; Sprandel, L. L.; Kern, C. W. *Adv. Chem. Phys.* **1978**, *37*, 305.
6. Dixon, R. N. *Trans. Faraday Soc.* **1964**, *60*, 1363.
7. Lee, J. S. *Bull. Kor. Chem. Soc.* **1994**, *15*, 228.
8. Estes, D.; Secrest, D. *Mol. Phys.* **1986**, *59*, 569.
9. Lee, J. S. *J. Chem. Phys.* **1992**, *97*, 7489.
10. Lee, J. S.; (submitted).

11. Bartholomae, R.; Martin, D.; Sutcliffe, B. T. *J. Mol. Spectrosc.* **1981**, *87*, 367.
12. Simons, G.; Parr, R. G.; Finlan, J. M. *J. Chem. Phys.* **1973**, *59*, 3229.
13. Lee, J. S.; Secrest, D. *J. Phys. Chem.* **1988**, *92*, 1821.
14. Renner, R. *Z. Physik* **1934**, *92*, 172.

Photochemical Intramolecular Diels-Alder Reactions of 1-Substituted Cyclopentadienes by Triplex Formation

Hyo Jung Yoon, Won Sik Chung, Bo Bin Jang, and Woo Ki Chae*

Department of Chemistry Education, Seoul National University, Seoul 151-742, Korea

Received May 23, 1995

In recent report, Schuster[1] *et al.* investigated the triplex Diels-Alder reaction to overcome [2+2] dimerization of diene to dienophile. According to Schuster's results, DCA (9,10-dicyanoanthracene)-sensitized irradiation of 5-alkenyl-1, 3-cyclohexadiene gives [4+2] adduct without isomerization to 1-alkenyl-1,3-cyclohexadiene prior to cyclization. 1-Substituted cyclopentadienes,[2] however, differing from 5-alkenylcyclohexadienes, [1,5]-hydrogen transfer is possible prior to cyclization producing two types of tricyclic adduct A and B (Scheme 1).

In this report, we wish to discuss spectroscopic implication of intramolecular triplex and the triplex effect on the product distribution from cyclization of the substituted cyclopentadienes 1 and 2.

1-(1,5-Dimethyl-4-hexenyl)cyclopentadiene (**1**) and 1-(5-Phenyl-*cis*-4-pentenyl)cyclopentadiene (**2**) were synthesized according to the reports by Fallis[3] and Wenkert[4] respectively.

Irradiation of DCA-saturated benzene solution of 1 and 2 at 350 nm give [4+2] adducts 3 and 5 as major products (eq. 1). The structures of 3 and 5 were identified by ^1H and ^{13}C NMR spectroscopy.[5] A consideration of ^{13}C DEPT

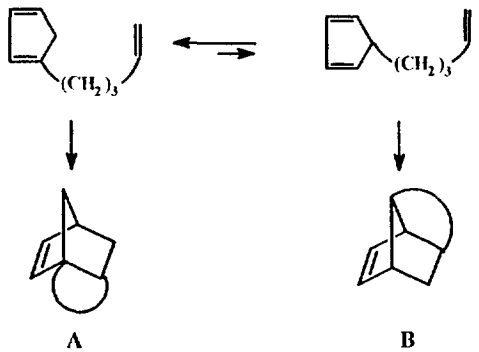

Scheme 1.

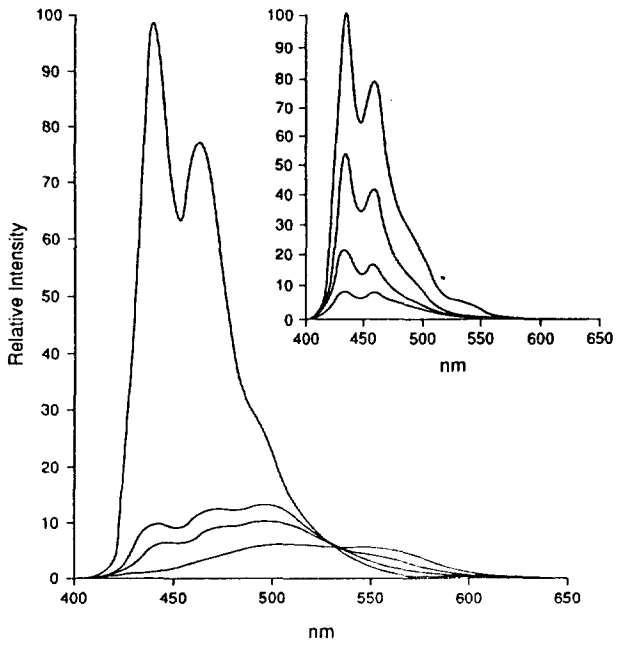

Figure 1. Fluorescence spectra of DCA with increasing concentration of *trans*-β-methylstyrene in benzene Insert : quenching of the DCA fluorescence with cyclopentadiene.

spectrum of 5 permits discrimination of the compound 5 and 6. One of the minor products formed in DCA-sensitized reactions of 1 and 2 seems to be [2+2] adduct by comparison with the major product obtained in the benzophenone-sensitized reactions. However, detailed identification procedures of these products were not performed.

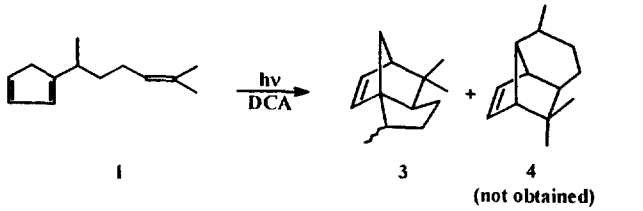

(1)

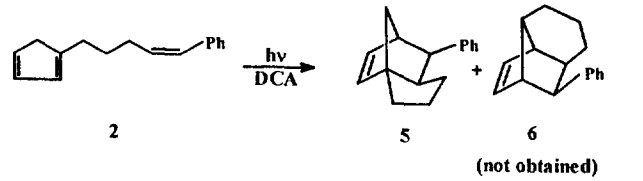

For a spectroscopic implication of the triplex formation, the DCA fluorescence was quenched by *trans*-β-methylstyrene and cyclopentadiene which are parts of the diene and dienophile in compound 2. Figure 1 shows the fluorescence of DCA in benzene solutions contaning increasing concentration of *trans*-β-methylstyrene. The broad, structureless emission with a maximum at 550 nm is assigned to the DCA-*trans*-β-methylstyrene exciplex.

However, the exciplex emission of the trienes 1 and 2 under any conditions were not detected. These results imply that exciplexes are formed in the case of these trienes but the concentration ratio of diene to dienophile is always 1